EUROPEAN ORGANIZATION FOR NUCLEAR RESEARCH

ON $K_L - K_S$ REGENERATION IN COPPER

A. Böhm*), P. Darriulat, C. Grosso**),
V. Kaftanov***), K. Kleinknecht, H.L. Lynch†),
C. Rubbia, H. Ticho††) and K. Tittel

CERN, Geneva, Switzerland.

ABSTRACT

The transmission regeneration amplitude after a thick copper block has been measured. The quantity $|f(0) - \bar{f}(0)|/k$ varies from 20.0 ± 1.4 mb at 2.75 GeV/c to 13.6 ± 1.2 mb at 7.25 GeV/c. Results are in excellent agreement with optical model calculations in which real and imaginary parts of the amplitudes for single nucleon scattering are determined from forward dispersion relations and total cross-sections.

Geneva - July 1967
(Submitted to Physics Letters)

*) Visitor from the III.Physikalisches Institut der Technischen Hochschule, Aachen.

**) Visitor from the Istituto di Fisica, Torino.

***) Visitor from the Institute of Theoretical and Experimental Physics, Moscow.

†) National Science Foundation (USA) Fellow.

††) J.S. Guggenheim Fellow, on leave from the University of California, Los Angeles.

The phenomenon of $K_L - K_S$ regeneration has been known since the work of Good et al.[1]. It consists of a transformation of an incident long-lived neutral K wave into a coherent superposition of the short- and long-lived states:

$$|K_L> \rightarrow |K_L> + \rho|K_S> .$$

Regeneration is expected to occur for any process in which K^0 and $\bar{K}^0$ states interact differently. In the present experiment, three main types of regeneration can be observed:

i) inelastic regenerative scattering in which the target nucleus is either excited or broken-up in the collision;

ii) elastic regenerative scattering in which the nucleons of the nucleus act coherently, yielding an angular distribution comparable to the one of elastic scattering;

iii) transmission regeneration, in which the whole block of matter, the "regenerator", recoils without phonon excitation. The process is somehow analogous to the rotation of the plane of polarization of ordinary light in an anisotropic medium. The angular distribution of the outgoing wave is a diffraction-like pattern with the first Fresnel zone at about 10^{-7} radians.

We have measured the energy dependence of process (iii) after a thick copper regenerator. The regenerated K_S intensity is measured by observing decays into the $\pi^+\pi^-$ mode immediately after the regenerator.

The transmission regenerated amplitude at the regenerator exit is given by[1]:

$$\rho = 2\pi \, i \, \Lambda_S \, N \times \frac{f(0) - \bar{f}(0)}{k} \times \frac{1 - e^{+(i\Delta m/\gamma_S - 1/2)\ell}}{1 - 2 \, i \, \Delta m/\gamma_S} \qquad (1)$$

where

$k = p/\hbar$ is the K_L wave number,

$\Lambda_S = \beta\gamma\tau_S$ is the mean decay length of the K_S,

N is the density of scattering centres,

$\Delta m = m_L - m_S$ is the K_L, K_S mass difference,

$\gamma_S = \hbar/\tau_S$ is the K_S decay width,

$\ell = L/\Lambda_S$ is the length of the regenerator in units of decay lengths,

$f(0)$ and $\bar{f}(0)$ are the K^0 and $\bar{K}^0$ elastic forward scattering amplitudes.

The only term in the expression that cannot be readily evaluated from the regenerator geometry and the well-known τ_S and Δm values is the difference between the K^0 and $\bar{K}^0$ forward scattering amplitudes, $f(0) - \bar{f}(0)$. We have evaluated the quantity $f(0) - \bar{f}(0)$ in a two-step calculation.

a) Firstly, the proton and neutron forward scattering amplitudes for K^0 and $\bar{K}^0$ have been determined from experimental data on charged kaons as a consequence of Isotopic Spin Symmetry. The imaginary part of the scattering amplitudes was determined with the optical theorem from available $K^{\pm}p$ and $K^{\pm}n$ total cross-section measurements[2]. Real parts are extracted from forward dispersion relations[3].

b) The regeneration amplitudes for a nucleus have been calculated from the nucleon amplitudes in the framework of an optical model[4-6]. We have chosen a nuclear density distribution equal to the charge distribution from electron scattering experiments.

The experimental data and prediction of the model are in excellent agreement.

1. THE EXPERIMENTAL METHOD

The 19.2 GeV/c extracted proton beam from the CERN Proton Synchrotron was focused on a 70 mm long tungsten target. A long-lived neutral beam was defined by a channel 2 × 5 cm² cross-section at an average angle of 140 mrad to the proton beam line. A vertical magnetic field of 36 kilogauss × meter swept away the charged particles. In order to eliminate γ-ray background, about 10 radiation lengths of lead were placed inside the channel.

Decays $K \to \pi^+\pi^-$ are detected with a magnetic spectrometer with optical spark chambers (Fig. 1). As in our previous work[7], the magnetic field integral in the spectrometer magnet was arranged so as to compensate the transverse momentum of the pion pair from the K^0 decay. Events in which both particles emerged parallel within about $\pm 2.3°$ after the magnet were selected by an eight-channel counter hodoscope. The normal trigger logic required in addition a veto condition at the anticoincidence counter in front of the decay volume, and a charged particle at each side of the decay volume in front of the first spark chamber before the magnet. Electrons from $K \to \pi e \nu$ decays were identified by a CO_2 threshold gas Čerenkov counter, 200 cm long, inserted between the first and second layers of the hodoscope counters. Muon signatures from $K \to \pi\mu\nu$ decays were obtained by a threefold scintillation counter coincidence after traversing an iron shield, 140 cm thick, corresponding to a threshold of 1.7 GeV/c. Muon signatures and Čerenkov pulse-heights were recorded directly on each picture.

The detection efficiency of the spectrometer is limited mainly by the usable width of the magnet (82 cm). Decays from slow K^0's are better detected if they originate near to the magnet. Therefore measurements were done for two positions of the regenerator and at distances of 398 cm and 256 cm from magnet centre. The K momentum ranges covered by these two positions overlap and extend from 2.5 to 7.5 GeV/c.

2. DATA ANALYSIS

Pictures were scanned and measured by a cathode-ray digitizer at the rate of about 1000 pictures/hour. Data were analysed to separate the 2π decays of transmission regenerated K_S and of incoming K_L from background events, namely:

i) $K_S \to \pi^+\pi^-$ from K_S scattered in the regenerator, and $K_S \to \pi^+\pi^-$ where the K_L has been scattered before undergoing regeneration;

ii) leptonic decays $K_L \to \pi e \nu$, $K_L \to \pi\mu\nu$;

iii) neutron stars in air, and other backgrounds.

The invariant mass $m_{\pi\pi}$ of the charged pair seen in the spectrometer, assuming both particles to be pions, and the angle ϑ_K between the reconstructed K momentum and the K_L line-of-flight are calculated; namely:

$$m_{\pi\pi} = \sqrt{(E_+ + E_-)^2 - (\vec{p}_+ + \vec{p}_-)^2}$$

$$\cos \vartheta_K = \frac{\vec{p}_{\pi\pi} \cdot \vec{u}_K}{|\vec{p}_{\pi\pi}| \; |\vec{u}_K|} ,$$

where $\vec{p}_{\pi\pi} = \vec{p}_+ + \vec{p}_-$, and $\vec{u}_K$ is a vector pointing in the direction of the neutral decaying particle.

The distribution in the square of the reconstructed K^0 angle ϑ_K^2 shows a very marked forward peak, corresponding to transmission regenerated events. The shape of the forward peak is in good agreement with the expected angular distribution of the incident K_L beam in which measurement errors on the charged decay particles are properly folded in. For a cut $\vartheta_K^2 < 3 \times 10^{-5}$, the loss of $K_S \to \pi^+\pi^-$ is less than 2% for the momenta considered. The mass distribution of the resulting sample is shown in Fig. 2a. Events in the region $488 < m < 508$ MeV are taken to be $K_S \to \pi^+\pi^-$. The background under the peak is about 2% and is estimated from the events outside this region. The background of events of type (i) after the angle cut is negligible. There are 1557 $K \to \pi^+\pi^-$ events for the upstream position, and 3552 $K \to \pi^+\pi^-$ events for the downstream position.

Next we calculate the time-of-flight in the K^0 rest frame from the exit of the regenerator to the decay point. The sample of $K \to 2\pi$ decay events is divided into (p,t) bins of 0.5 GeV/c and 5×10^{-11} sec size, and compared with the expected distribution function in which also the effects due to $K_L \to \pi^+\pi^-$ decay amplitude are included:

$$N(p,t) = \beta \, S(p) \, \epsilon(p,t) \, e^{-\Gamma_S t} \, |\rho(p)|^2 \left\{ 1.0 + 2\left|\frac{\eta}{\rho(p)}\right| e^{\Gamma_S t/2} \cos(\Delta m t - \varphi) + \right.$$

$$\left. + \left|\frac{\eta}{\rho(p)}\right|^2 e^{\Gamma_S t} \right\} ,$$

where:

$S(p)$ is the incident K_L momentum spectrum, measured in Ref. 7,

$\epsilon(p,t)$ is the detection efficiency obtained by Monte Carlo calculations in which measurement errors and multiple scattering in the detector are taken into proper account,

η is $\dfrac{\text{Amplitude } K_L \to \pi^+\pi^-}{\text{Amplitude } K_S \to \pi^+\pi^-}$,

$\rho(p)$ is the regeneration amplitude,

β is an over-all normalization constant, and

φ is defined as $[\arg(\eta_{+-}) - \arg(\rho(p)]$.

Since for the present case $|\eta/\rho(p)| \sim 1/40$, terms of order $|\eta/\rho(p)|$, and $|\eta/\rho(p)|^2$ are small, they can be safely handled as corrections.

From Formula (1) we get:

$$\arg(\rho) = \arg\{i[f(0) - \bar{f}(0)]\} + \arg\left[\frac{1 - e^{+(i\Delta m/\gamma_S - 1/2)\ell}}{1 - 2i\,\Delta m/\gamma_S}\right].$$

The phase $\arg(\eta) - \arg\{i[f(0) - \bar{f}(0)]\}$ is known from previous work[8] to be $+1.42 \pm 0.18$ rad at $p_K = 2.80$ GeV/c. On the basis of the expected smooth variation of $\arg\{i[f(0) - \bar{f}(0)]\}$ with momentum (Section 6) we have set $\arg\{i[f(0) - \bar{f}(0)]\} = \text{const.}$ Results have been found to be completely insensitive to substantial changes in the value of this phase.

3. NORMALIZATION

The regeneration intensity is normalized to the kinematically identical decay process $K_L \to \pi^+\pi^-$ observed in a separate run without regenerator. The ratio between the effective K_L fluxes in exposures with and without regenerator is determined from a sample of $K_L \to \pi^\mp e^\pm \nu$ events observed in a fixed decay region several K_S lifetimes away from the regenerators.

In order to minimize regeneration effects from the collimator edges, decays $K_L \to \pi^+\pi^-$ occurring at less than eight K_S lifetimes from the end of the beam-defining channel have been discarded. The invariant mass of this sample in the forward peak $\vartheta_K^2 < 3 \times 10^{-5}$ is shown in Fig. 2b. Most of K_{e3} decays are removed from the sample by means of the gas-Čerenkov signature, and the background consists mainly of $K_{\mu 3}$ decays which cannot be detected behind the Fe wall (average K momentum is $\sim$ 3 GeV/c). The background under the mass peak around m_K has been obtained by interpolating the shape of the $K_{\mu 3}$ mass distribution. A total of 1183 ± 100 events are retained.

The relative normalization of these $K_L \to \pi^+\pi^-$ decays to the sample behind the regenerators is determined from the number of $K_L \to \pi e \nu$ decays where the electron is detected by the Čerenkov counter. The vertex distribution of K_{e3} events behind the regenerators is shown in Fig. 3 and compared to the same distribution without regenerator. The subtraction of leptonic decays from kaons scattered in the regenerator is taken into account by dividing the number of events by the factor

$$1 + \sum_{i=1}^{\infty} (N \sigma_D L)^i \frac{\epsilon_i}{\epsilon_0} \quad ,$$

where

$N = 8.45 \times 10^{22}$ atoms/cm^3,

$\sigma_D = 0.28$ barn [9] is the diffraction cross-section,

$L = 20$ cm is the length of the regenerator, and

ϵ_i is the K_{e3} efficiency for a K_L which scattered i times.

4. EXPERIMENTAL RESULTS

Measured values for the quantity $|f(0) - \bar{f}(0)|/k$ are reported in Fig. 4. In addition to the statistical error, a scale error of 6% is added because of:

i) uncertainties in the value of $|\eta| = 1.96 \pm 0.06 \times 10^{-3}$;

ii) errors in the number of $K_L \to \pi^+\pi^-$ recorded in the run with no regenerator (5%);

iii) statistical error in the number of leptonic counts (2%); and

iv) error in the diffraction correction (2.5%) in the $K \to \pi e \nu$ event samples.

The quantity $|f(0) - \bar{f}(0)|/k$ after an initial drop becomes essentially constant for momenta above 5 GeV/c: it varies from 20.0 ± 1.4 mbarn at 2.75 GeV/c to 13.6 ± 1.2 mbarn at 7.25 GeV/c.

Results appear to be consistent with the recently published work of Bennett et al.[9] and with the measurements of Christenson et al.[10] at p = 1.1 GeV/c.

5. OPTICAL MODEL CALCULATION

Let us denote with $a^p(0)$, $a^n(0)$ the forward scattering amplitudes for K° in protons and neutrons, respectively. From the Optical Theorem and charge symmetry of strong interaction, it follows that

$$\text{Im}\,[a^p(0)] = \frac{k}{4\pi}\,\sigma_T(K^\circ p) = \frac{k}{4\pi}\,\sigma_T(K^+ n)$$

$$\text{Im}\,[a^n(0)] = \frac{k}{4\pi}\,\sigma_T(K^\circ n) = \frac{k}{4\pi}\,\sigma_T(K^+ p)\ ,$$

where we denote with σ_T the total cross-sections. Analogous relationships are valid for $\bar{K}^\circ$.

Real parts of the forward scattering amplitudes, Re $[a^p(0)]$, Re $[a^n(0)]$, can be obtained with the help of the forward dispersion relationships from an integral over total cross-sections. We have taken the results of Lusignoli et al.[3], who have evaluated the real parts of $K^\pm p$ and $K^\pm n$ forward scattering amplitudes. Results for $K^- p$ and $K^- n$ are compatible with zero for K momenta > 2.0 GeV/c. Those authors also find that in the momentum interval 2.0 GeV/c < p_K < 7.0 GeV/c, the quantities (Re/Im)$(K^+ p)$ vary from -0.6 to -0.3 and (Re/Im)$(K^+ n)$ from -0.3 to -0.1.

The corresponding scattering amplitudes for a copper nucleus are calculated as the resultant of the proton and neutron contributions evaluated in the framework of an optical model calculation[4-6]. If we indicate with k_0 the wave number for a free particle, then in nuclear matter

$$k(\vec{r}) = k_0 + k'(\vec{r}) \ .$$

The optical model gives

$$k'(\vec{r}) = \frac{2\pi R(\vec{r})}{k_0} \ \frac{1}{A}\left[Z\ a^p(0) + (A - Z)\ a^n(0)\right].$$

where $R(\vec{r})$ is the nuclear density distribution.

Now define

$$P(b) = \int_{-\infty}^{+\infty} k'(\vec{r})\ ds =$$

$$= \frac{1}{A}\left[Z\ a^p(0) + (A - Z)a^n(0)\right]\frac{4\pi}{k_0}\int_0^{\infty} R\left(\sqrt{s^2 + b^2}\right) ds, \qquad (2)$$

where b is the impact parameter and s the variable along the path of the particle across the potential. The integral can be considered as weighted path length of the particle through the matter. Then in the plane-wave Born approximation the scattering amplitude is

$$\text{for } K_0 \ : \ f(\vartheta) = i\ k_0 \int_0^{\infty} \{1 - \exp\left[i\ P(b)\right]\} J_0\ (k_0 b \sin\vartheta)\ bdb \qquad (3)$$

$$\bar{K}_0 \ : \ \bar{f}(\vartheta) = i\ k_0 \int_0^{\infty} \{1 - \exp\left[i\ \bar{P}(b)\right]\} J_0\ (k_0 b \sin\vartheta)\ bdb\ , \qquad (4)$$

where J_0 is the usual Bessel function and $\bar{P}(b)$ is the integral (2) for an incident $\bar{K}^0$ state.

The calculation has been done taking a two-parameter Fermi distribution for the density function

$$R(\vec{r}) = R_0 / \{1 + \exp [(r - c)/d]\} ,$$

where $d = 0.57 \pm 0.02$ Fermi is the diffuseness parameter, and

$c = 4.23 \pm 0.04$ Fermi is the half-density radius,

obtained from electron scattering experiments[11].

The results of the calculation are shown in Fig. 4, where the error bands take into account only the uncertainties in the determination of the scattering amplitudes on protons and neutrons.

The calculated results on the transmission regeneration amplitudes are in very good agreement with the experimental data. The fall-off of the real parts of K^+p and K^+n amplitudes and the variation of the total cross-sections contribute about equally to the observed decrease of the quantity $|f(0) - \bar{f}(0)|/k$ towards higher momenta.

6. OTHER PREDICTIONS OF THE MODEL

The optical model yields additional predictions:

1) The phase of the regeneration amplitude for a very thin regenerator is given by

$$\varphi_f = \arg \{i[f(0) - \bar{f}(0)]\}.$$

The prediction for φ_f is given in Fig. 5, and it is in good agreement with the measurement of Bennett et al.[12] for $m_L > m_S$. If, instead, $m_L < m_S$, the experimental result and the optical model calculation would have opposite signs. Therefore the conclusion of direct measurements[13,14], which favour the alternative $m_L > m_S$, is confirmed.

2) The differential cross-section for elastic regenerative scattering on nuclei is given by[1]

$$\frac{d\sigma}{d\Omega}(\vartheta) = \frac{1}{4} |f(\vartheta) - \bar{f}(\vartheta)|^2 .$$

For small angles it can be well approximated by a Gaussian distribution $|f(\vartheta) - \bar{f}(\vartheta)|^2 \sim e^{-(p\vartheta/p^*_R)^2}$, corresponding to a diffraction-like process. The model gives the prediction $p^*_R = 68$ MeV/c, about 12% smaller than the corresponding parameter for non-regenerative scattering $p^* = 76.5$ MeV/c. The somewhat steeper fall-off of the angular distribution of regenerated events can be understood by the fact that the difference between nuclear transparencies for K_0 and $\bar{K}_0$ is largest around the "RIM" of the nucleus. The "effective" nuclear radius for regenerative scattering is therefore correspondingly larger.

Acknowledgements

We wish to express our thanks to several of our colleagues in CERN, and especially to Professor Jack Sandweiss for many interesting remarks.

REFERENCES

1) R.H. Good, R.P. Matsen, F. Muller, O. Piccioni, M.W. Powell, H.S. White, W.B. Fowler and R.W. Birge, Phys.Rev. 124, 1223 (1961).

2) R.L. Cool, G. Giacomelli, T.F. Kycia, B.A Leontic, K.K. Li, A. Lundby and F. Teiger, Phys.Rev.Letters 16, 1228 (1966); Phys.Rev.Letters 17, 102 (1966);

W.F. Baker, E.W. Jenkins, T.F. Kycia, R.H. Phillips, A.L. Read, K.F. Riley and H. Ruderman, Proc.Sienna Int.Conf. on Elementary Particles (Società Italiana di Fisica, Bologna, Italy, 1963), p. 634;

W.F. Baker, R.L. Cool, E.W. Jenkins, T.F. Kycia, R.H. Phillips and A.L. Read, Phys.Rev. 129, 2285 (1963);

H.C. Burrowes, D.O. Caldwell, D.H. Frisch, D.A. Hill, D.M. Ritson and R.A. Schluter, Phys.Rev.Letters 2, 117 (1959);

O. Chamberlain, K.M. Crowe, D. Keefe, L.T. Kerth, A. Lemonick, Tin Maung and T.F. Zipf, Phys.Rev. 125, 1696 (1962);

V. Cook, Bruce Cork, T.H. Hoang, D. Keefe, L.T. Kerth, W.A. Wenzel and T.F. Zipf, Phys.Rev. 123, 320 (1961);

V. Cook, D. Keefe, L.T. Kerth, P.G. Murphy, W.A. Wenzel and T.F. Zipf, Phys.Rev.Letters 7, 182 (1961);

A.N. Diddens, E.W. Jenkins, T.F. Kycia and K.F. Riley, Phys.Rev. 132, 2721 (1963);

M. Ferro-Luzzi, R.D. Tripp and M.B. Watson, Phys.Rev.Letters 8, 28 (1962);

W. Galbraith, E.W. Jenkins, T.F. Kycia, B.A. Leontic, R.H. Phillips, A.L. Read and R. Rubinstein, Phys.Rev. 138, B913 (1965);

P. Nordin, Jr., Phys.Rev. 123, 2168 (1961);

W. Slater, D.H. Stork, H.K. Ticho, W. Lee, W. Chinowsky, G. Goldhaber, S. Goldhaber and T. O'Halloran, Phys.Rev.Letters 7, 378 (1961);

S. Goldhaber, W. Chinowsky, G. Goldhaber, W. Lee, T. O'Halloran, T.F. Stubbs, G.M. Pjerrou, D.H. Stork and H.K. Ticho, Phys.Rev. Letters 9, 135 (1962);

V.J. Stenger, W.E. Slater, D.H. Stork, H.K. Ticho, G. Goldhaber and S. Goldhaber, Phys.Rev. 134, B1111 (1964).

3) M. Lusignoli, M. Restignoli, G.A. Snow and G. Violini, Nuovo Cimento 45A, 792 (1966); Nuovo Cimento 49A, 705 (1967).

4) S. Fernbach, R. Serber and T.B. Taylor, Phys.Rev. 75, 1352 (1949).

5) K.M. Watson, Phys.Rev. 89, 575 (1953); Phys.Rev. 105, 1388 (1957).

6) J.W. Cronin, R.L. Cool and A. Abashian, Phys.Rev. 107, 1121 (1957).

7) A. Böhm, P. Darriulat, C. Grosso, V. Kaftanov, K. Kleinknecht, H.L. Lynch, C. Rubbia, H. Ticho and K. Tittel, Phys.Letters, in press.

8) C. Alff-Steinberger, W. Heuer, K. Kleinknecht, C. Rubbia, A. Scribano, J. Steinberger, M.J. Tannenbaum and K. Tittel, Phys.Letters 20, 207 (1966); Phys.Letters 21, 595 (1966).

9) S. Bennett, D. Nygren, H. Saal, J. Sunderland, J. Steinberger and K. Kleinknecht, Phys.Letters 27B, 244 (1968).

10) J.H. Christenson, J.W. Cronin, V.L. Fitch and R. Turlay, Phys.Rev. 140B, 74 (1965).

11) R. Hofstadter and H.R. Collard, in Landolt-Börnstein, New Series I, Volume 2 Nuclear Radii, (Springer Verlag, 1967).

12) S. Bennett, D. Nygren, H. Saal, J. Sunderland and J. Steinberger, Phys.Letters 27B, 239 (1968).

13) W.A.W. Mehlhop, S.S. Murty, P. Bowles, T.H. Burnett, R.H. Good, C.H. Holland, O. Piccioni and R.A. Swanson, University of California, San Diego, preprint April 1968.

14) J. Canter, T. Cho, A. Engler, H.E. Fisk, R.W. Kraemer, C.M. Meltzer, D.G. Hill, D.K. Robinson and M. Sakitt, Phys.Rev.Letters 17, 942 (1967).

Table

Regeneration amplitude as a function of K momentum

Momentum GeV/c	$\lvert f(0) - \bar{f}(0)\rvert / k$ mb
2.75	20.0 ± 1.4
3.25	18.2 ± 1.2
3.75	16.4 ± 1.0
4.25	16.4 ± 1.0
4.75	16.0 ± 1.0
5.25	14.7 ± 1.0
5.75	15.2 ± 1.0
6.25	13.2 ± 1.1
6.75	14.4 ± 1.2
7.25	13.6 ± 1.2

Figure captions

Fig. 1 : Layout of the experimental arrangement.

Fig. 2a : Invariant mass distribution of particle pairs (assumed to be pions) for the regenerator events. Only events for which the angle between the reconstructed momentum and the K_L line-of-flight is $\vartheta_K^2 \leq 3 \times 10^{-5}$ are retained.

Fig. 2b : Some distribution as in Fig. 2a for events collected with no regenerator in the beam.

Fig. 3 : Vertex distribution of $K \to \pi^{\pm} e^{\mp} \nu$ events used to determine the normalization constants between runs, with and without regenerators.

Fig. 4 : Regeneration amplitude for copper. Experimental points are compared with the predictions of the optical model calculations. Dashed lines are indicating the uncertainties in the total cross-section measurements and in the forward dispersion relationships on free nucleons.

Fig. 5 : Energy dependence of the regeneration phase in copper. The experimental point is taken from the paper of Bennett et al.[9]. The dashed lines have the same meaning as in Fig. 4.

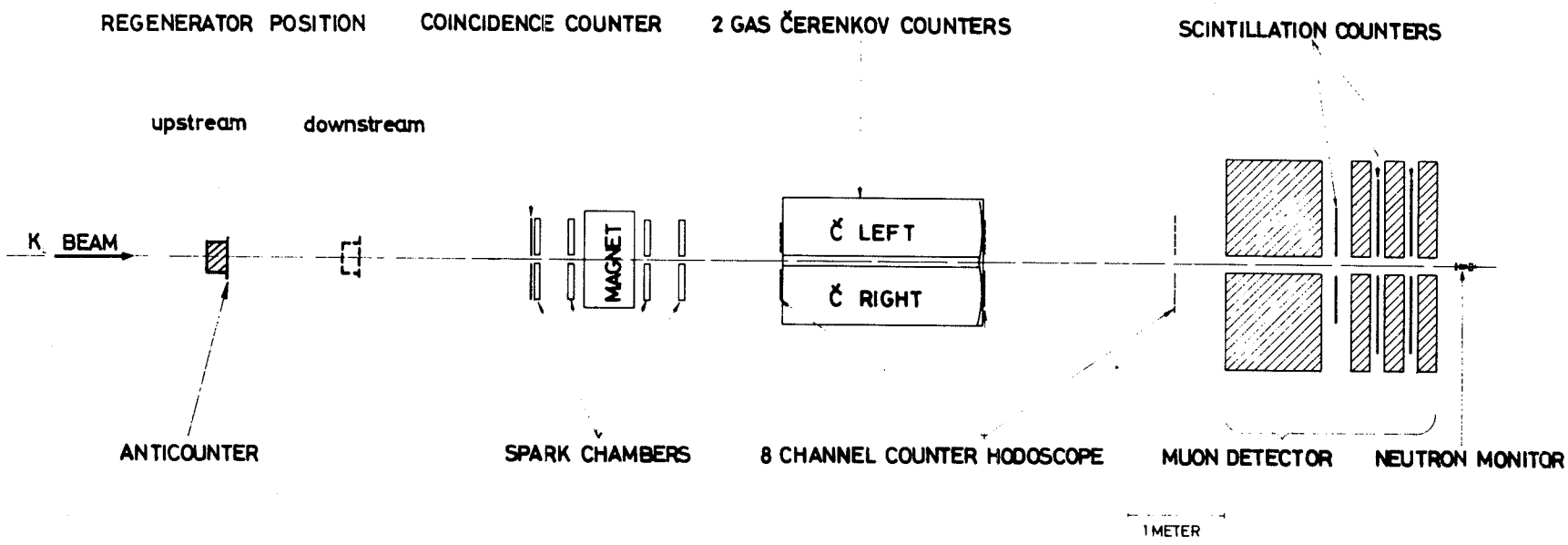
REGENERATOR POSITION
COINCIDENCE COUNTER
2 GAS ČERENKOV COUNTERS
SCINTILLATION COUNTERS
upstream
downstream
K BEAM
MAGNET
Č LEFT
Č RIGHT
ANTICOUNTER
SPARK CHAMBERS
8 CHANNEL COUNTER HODOSCOPE
MUON DETECTOR
NEUTRON MONITOR
1 METER

Fig. 1

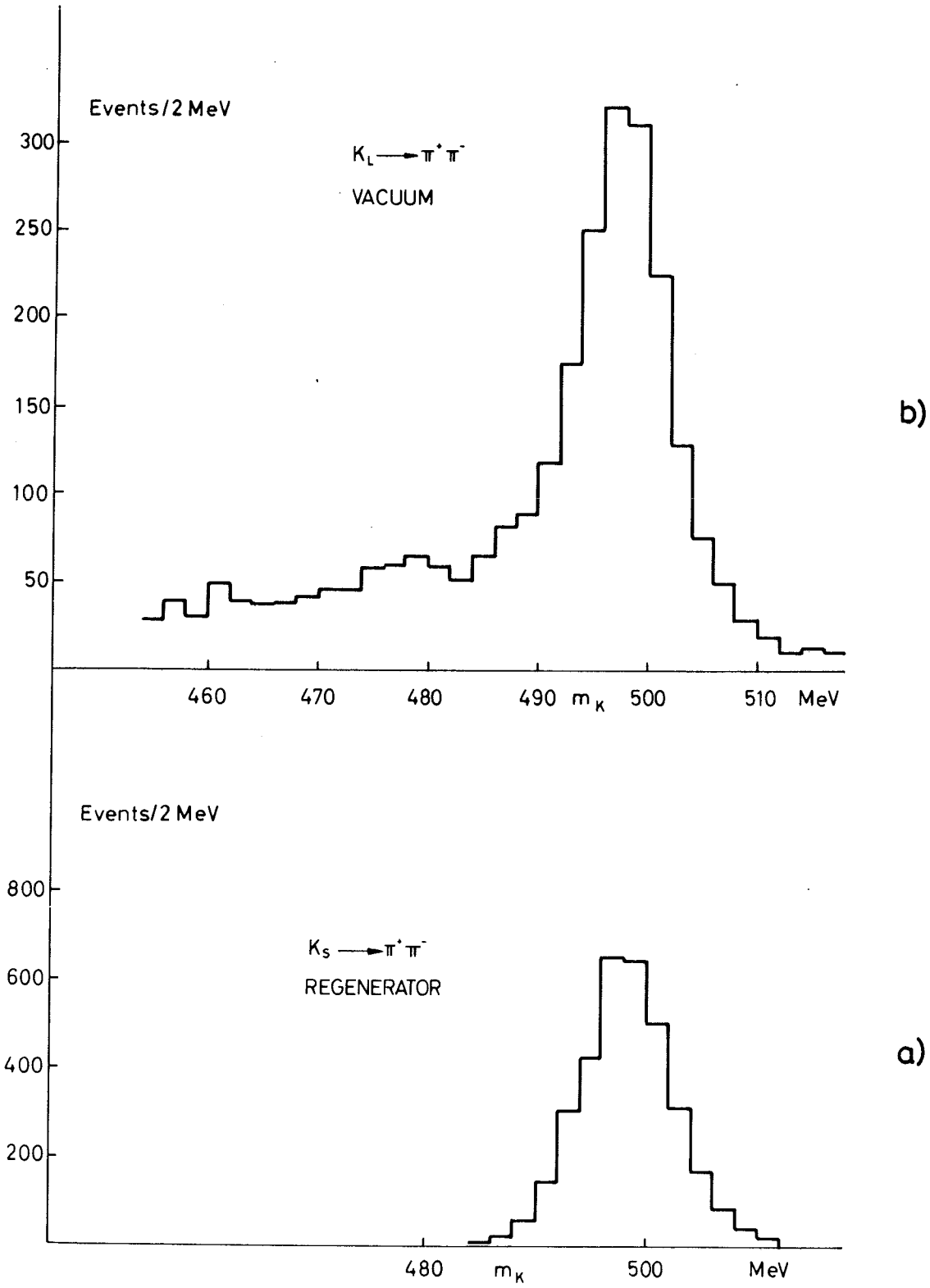
Events/2 MeV
300
250
200
150
100
50
$K_L \longrightarrow \pi^+\pi^-$
VACUUM
460
470
480
490
m_K
500
510
MeV
b)
Events/2 MeV
800
600
400
200
$K_S \longrightarrow \pi^+\pi^-$
REGENERATOR
480
m_K
500
MeV
a)

Fig. 2

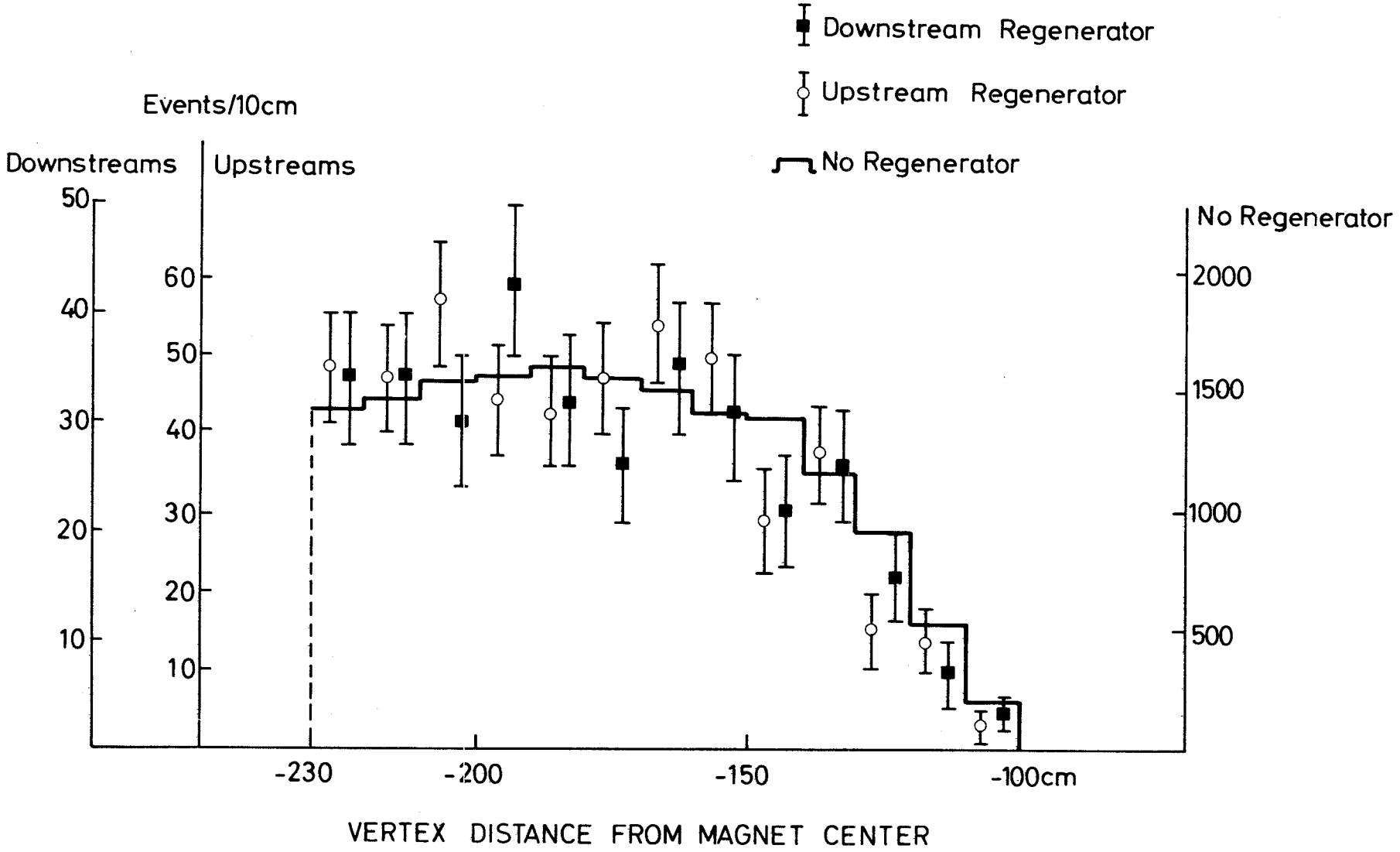
Downstream Regenerator
Upstream Regenerator
No Regenerator
Events/10cm
Downstreams
Upstreams
No Regenerator
50
40
30
20
10
60
50
40
30
20
10
2000
1500
1000
500
-230
-200
-150
-100cm
VERTEX DISTANCE FROM MAGNET CENTER

Fig. 3

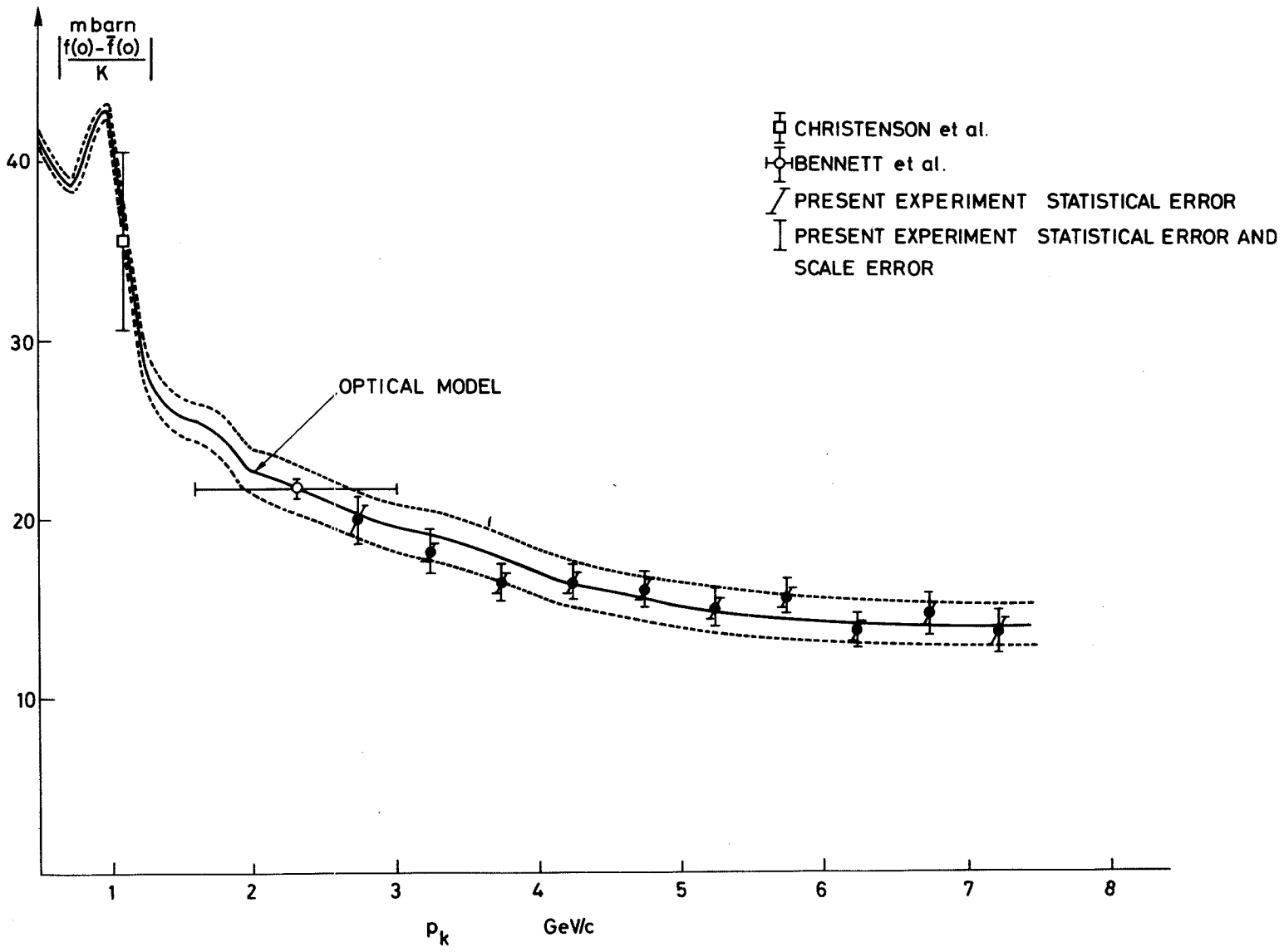
REGENERATION AMPLITUDE FOR COPPER
mbarn
|f(o)-f̄(o)/K|
40
30
20
10
CHRISTENSON et al.
BENNETT et al.
PRESENT EXPERIMENT STATISTICAL ERROR
PRESENT EXPERIMENT STATISTICAL ERROR AND SCALE ERROR
OPTICAL MODEL
1
2
3
4
5
6
7
8
p_k
GeV/c

Fig. 4

REGENERATION PHASE φ_f FOR COPPER

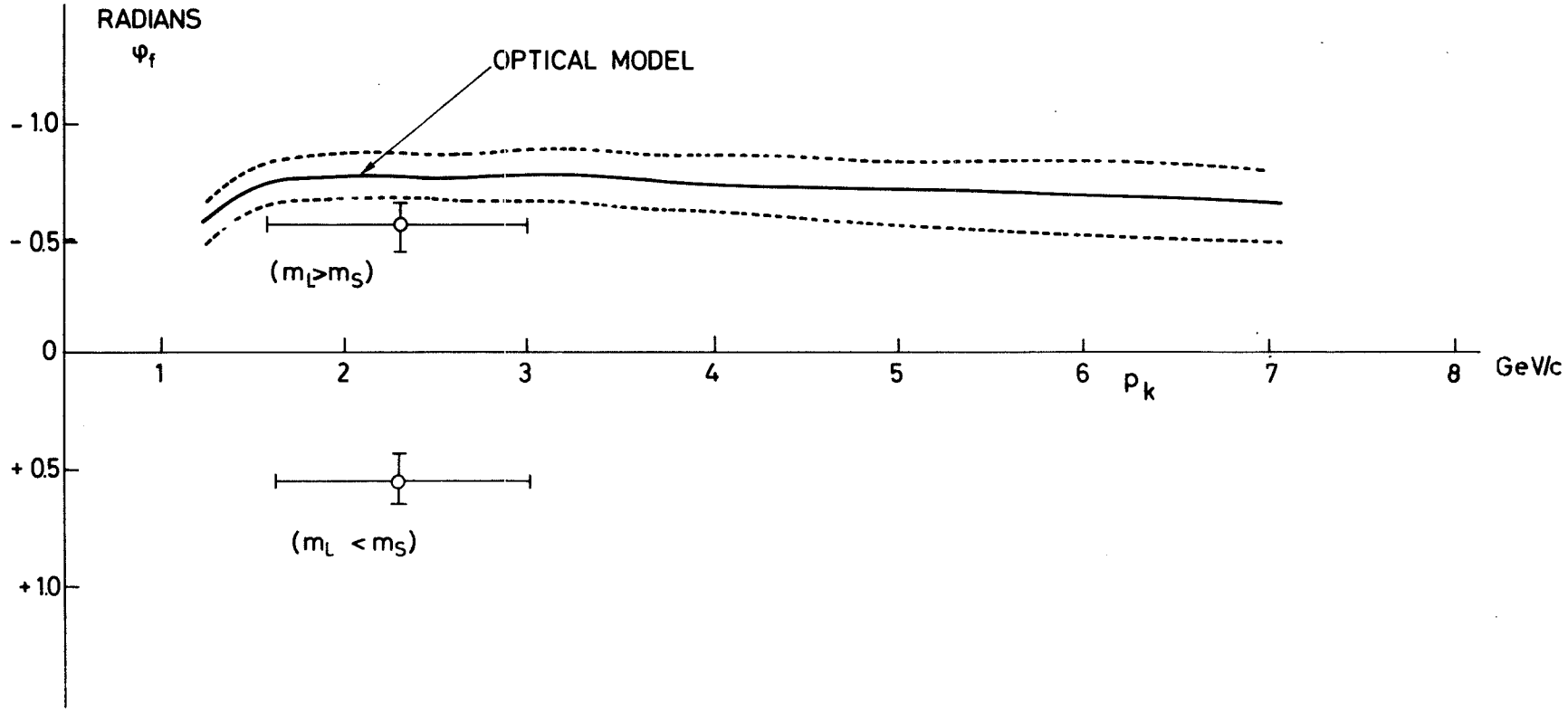

Fig. 5